

**THERMAL CHARACTERISTICS OF INCLINED WATER JET COOLING  
SYSTEM.**

**Raj Singh**

Research Scholar, Glocal University, UP, India  
[rsingh2019@yahoo.in](mailto:rsingh2019@yahoo.in)

**Y. P. Singh**

Supervisor / Guide, Glocal University India.  
[ypsingh14@gmail.com](mailto:ypsingh14@gmail.com)

**Milind Shivaji Rohokale**

Co-Guide, Principal- SKN Sinhgad Institute of Technology & Science  
Lonavala, Tal. Maval, Dist. Pune, PIN 410401, MH, India.  
[rohokalemilind74@gmail.com](mailto:rohokalemilind74@gmail.com)

**Abstract**

High-pressure water jet technology is currently highly significant in the automotive cleaning sector. Due to an inappropriate arrangement of nozzles on their spray rods, certain automated washers are unable to fulfill the washing requirements throughout the washing process. In this study, the internal and exterior flow field models of the nozzle are created using the computational fluid dynamics (CFD) theory. The flow field is simulated and examined using Fluent, and the external nozzle settings on the side spray bar of the automatic car washer are optimized. According to the modeling findings, when the nozzle and the normal line of the automotive surface are angled at a specific angle, the target surface is also subjected to tangential pushing force in addition to normal hitting force, which makes stains easier to remove. The nozzle should be angled away from the typical line of the automotive surface by 30° for the greatest washing results. The dynamic pressure on the surface of the car will rise as the nozzle inlet pressure rises, but after reaching a certain pressure, the rise in dynamic pressure will fall. The region that the water jet covers is not significantly impacted by the inlet pressure. In addition to completely covering and cleaning the automobile surface, the reasonable matching results of jet angle, nozzle spacing, and nozzle distance from the automobile surface (target distance) obtained by numerical simulation can also ensure less jet interference and no water waste from nearby nozzles. The aforementioned study findings can serve as a fundamental theoretical foundation for the best automatic car washing design.

**Key:** Thermal, Characteristics, Inclined, Water, Jet, Cooling, System, nozzle spacing.

**Introduction**

In the past, manual washing could not meet this large number and high frequency of automobile washing. At present, automatic automobile washing is divided into contact type and noncontact type. Although contact type can quickly remove stains on the automobile, hard particles (such as sand, small stones, and fine steel wires) often contained in stains on the automobile will get involved in the washing head, which results in the damage to the automobile.

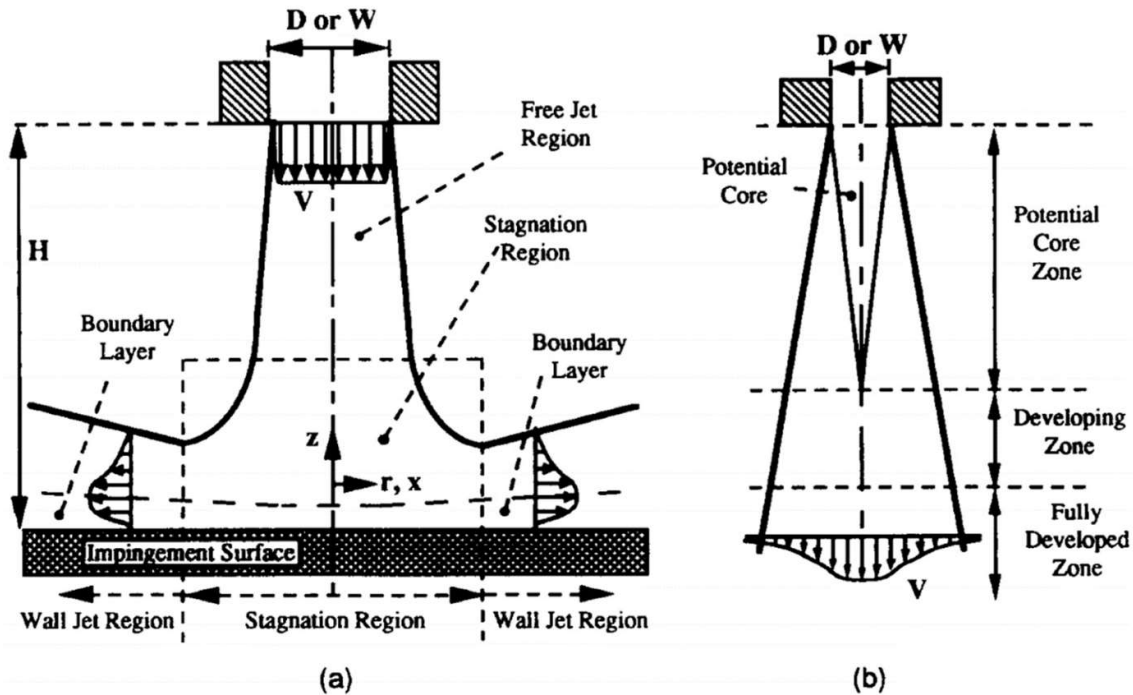


Fig.1: Thermal Characteristics of Inclined Water Jet Cooling System.

The noncontact type uses high-pressure water sprayed by high-pressure fan-type nozzles for washing, which will not cause friction damage to the automobile. High-pressure water jet washing is the key technology of automobile washer [4, 5]. It has been widely used because of its strong decontamination capability, wide application range, no environmental pollution, and easy automation [6–10]. It provides the basis for the automatic control of the car washing industry [11–14]. The high-pressure jet washer uses the high-pressure pump to provide pressure, and the high-pressure water flow is ejected from the nozzle [8, 15, 16].

Fuchs et al. [22] studied two different pulsating washing methods from the perspective of washing efficiency, thus reducing washing cost and saving operation time. Chee et al. [23] quantitatively analyzed the influence of jet length and wall curvature on the flow pattern of impinging water jet and preliminarily studied the jet washing effect. The length of time required to establish a stable flow is described. Nie et al. [24] obtained through numerical simulation that the jet impact pressure is larger when the nozzle outlet diameter is 2–7 times. Kermanpur et al. [25, 26] showed that, combined with industrial data and using the artificial neural network model, the sensitivity analysis of the influence of different injection angles, pressures, vertical heights, and water flow rates of phosphorus removal nozzles on jet striking force was carried out. In the range of 7 times the outlet diameter, the impact pressure is significantly reduced. Dou et al. [27] proposed a new type of self-propelled nozzle suitable for pipeline washing, analyzed the influence of the number, included angle, and eccentricity of nozzles on the pipeline washing effect, and proposed a reasonable arrangement to improve the efficiency of high-pressure water washing. In order to achieve the best washing effect, Liu et al. [28] carried out experimental research and analysis on the working state of the nozzle under different flow rates, from four aspects: cavitation form, pressure pulse frequency, velocity fluctuation

amplitude, and erosion effect. In order to understand the influence of structural parameters of high-pressure water jet nozzle on jet performance, the influence of various structural parameters of nozzle on jet performance was simulated and verified by experiments with outlet expansion angle, cone hole depth, and inlet contraction angle as reference factors and injection angle and jet flow rate as evaluation indexes by Liang and Gao [29]. For the sake of research on the effects of the inclination angle of forward nozzles and standoff distance, Liu et al. [30] adopted the ANSYS Fluent combined with RNG turbulence model to analyze the multinozzle jets flow field. The results indicate that the components of axial velocity and tangential velocity of forward nozzle jets are different from inclination angles of forward nozzles.

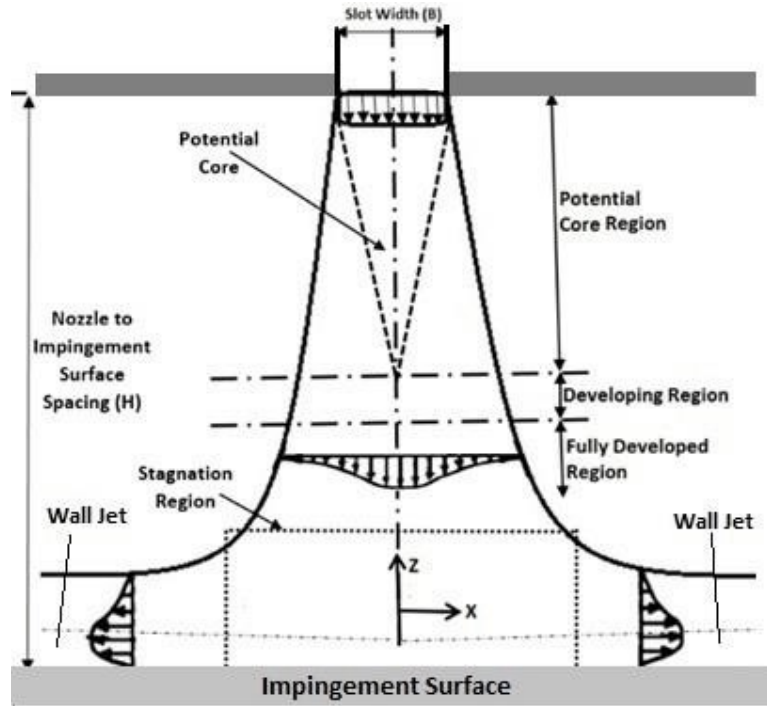


Fig.2: Thermal Characteristics of Inclined Water Jet Cooling System Process

At present, there are many researches on the influence of the internal structural parameters of the washing nozzle on its washing effect at home and abroad, but there are few researches on the influence of the external parameters of the fan-type nozzle for washing on its jet performance. However, in the actual application process, the washing effect of the high-pressure water jet on the automobile also depends on the distance between the nozzle and the automobile, the water flow pressure, the nozzle arrangement distance, the included angle between the nozzle and the normal line of the target surface, and so on.

### Mathematical Model of Nozzle Water Jet

Figure 1 is a physical diagram of the spray rod and nozzle of an automatic automobile washer. The nozzle water jet structure [31] is shown in Figure 2. After the water jet is ejected from the slit of the nozzle, due to the huge speed difference between the water jet and the surrounding

air and the exchange of energy and mass with the air, the ejected water jet continuously diffuses to the surrounding. Then the boundary of the jet widens, the velocity decreases, and the area where the velocity keeps the initial velocity unchanged also decreases continuously. The boundary with zero velocity is the outer boundary of the jet.



Fig 3 : The physical diagram of the side spray bar of an automatic automobile washer.

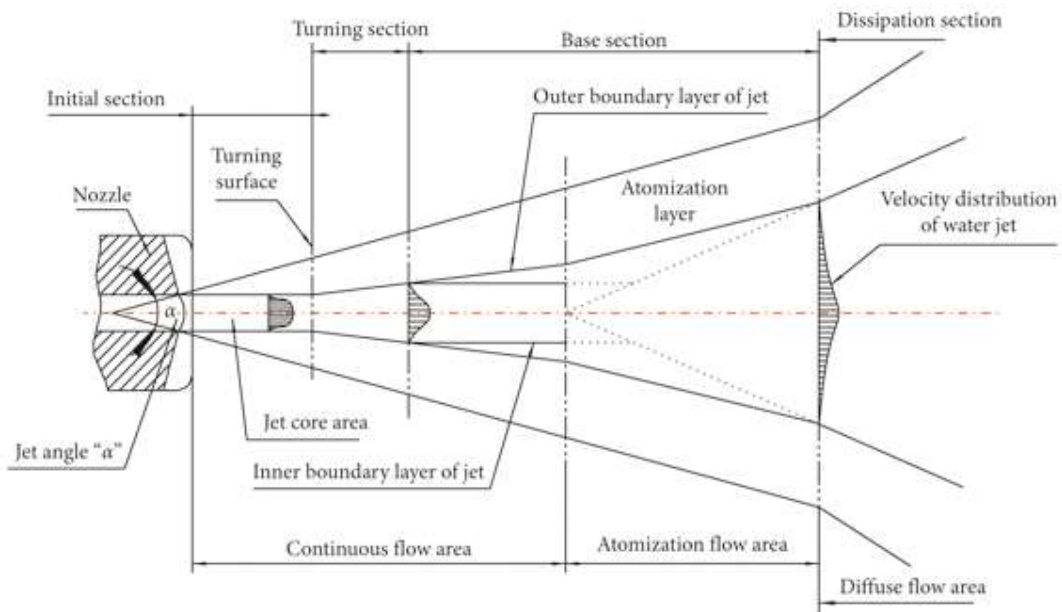


Fig 4 : The jet distribution structure diagram of the nozzle.

The water jet is roughly divided into three jet sections, which are successively divided into the initial section, the basic section, and the dissipation section from the nozzle outlet. The initial section of water jet is the jet section from the outlet of the nozzle to the complete disappearance of the velocity core. The axial dynamic pressure, velocity, and density remain basically unchanged in the jet core area.

### Mathematical Model

For high-pressure water jet washing, assuming that water is an incompressible steady-state flow, the continuity equation is where  $u$ ,  $v$ , and  $w$  are the three velocity components of  $x$ ,  $y$ , and  $z$ , respectively, m/s. The momentum equation is where  $f_x$ ,  $f_y$ , and  $f_z$  are the components of unit mass force on 3 coordinate axes, respectively;  $\rho$  is the density of water, kg/m<sup>3</sup>;  $\mu$  is the dynamic viscosity of water, kg/m·s. Water jet automobile washing belongs to the gas-liquid two-phase flow movement. First of all, it is necessary to judge whether it is a laminar flow or turbulent flow. In multiphase flow, each relevant parameter can be expressed by the following equation: where  $R_e$  is the Reynolds number;  $u_0$  is the velocity of water at the nozzle inlet, m/s, generally about 100 m/s;  $D$  is the diameter of nozzle inlet, about 3 mm;  $\mu = 0.001$  kg/m·s.

Substituting various data,  $R_e$  is 229400, which is much greater than 2300, so this jet belongs to highly turbulent flow. The standard  $k-\varepsilon$  is selected as the turbulence calculation model. The relevant calculation equation is as follows: where  $G_k$  is the turbulent kinetic energy generated by the laminar velocity gradient;  $G_b$  is the turbulent energy generated by the buoyancy;  $Y_M$  is the wave generated by the transition diffusion in the compressible turbulence;  $S_k$  and  $S_\varepsilon$  are user-defined source terms;  $C_{1\varepsilon}$ ,  $C_{2\varepsilon}$ , and  $C_{3\varepsilon}$  are the viscous diffusion coefficients (empirical constants), which are, respectively, 1.44, 1.92, and 0.09;  $\delta_k$  is the Prandtl number corresponding to the turbulent kinetic energy  $k$ ,  $\delta_k = 10$ ;  $\delta_\varepsilon$  is the Prandtl number corresponding to dissipation rate,  $\delta_\varepsilon = 1.3$ ;  $\mu_t$  is turbulent viscosity,  $\mu_t = \rho C_\mu k^2/\varepsilon$  [32].

### Establishment Simulation Model

The high-pressure water jet discussed in this paper belongs to obvious gas-liquid two-phase flow with obvious interface stratification, and the jet also belongs to free-surface flow. Based on the above mathematical model, VOF model and standard turbulent  $k-\varepsilon$  model are selected for analysis in simulation.

In order to study the water-gas two-phase flow field when the water jet leaves the nozzle and enters the air, SOLIDWORKS software is used to carry out 3D model of the internal and external flow fields. In order to better connect the internal flow fields with the external flow fields, a triangular prism is established outside the fan-type nozzle as the transition area of the internal and external flow fields [15], and the 3D model is shown in Figure 3.

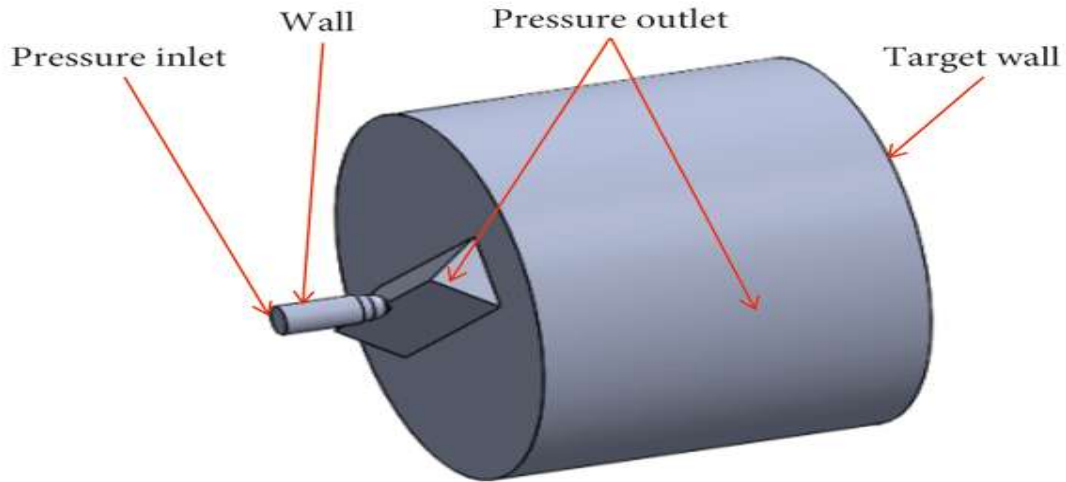


Figure 5: 3D model of nozzle and external flow field.

### 3.2. Mesh Generation and Fluent Boundary Condition Setting

In the process of mesh division, tetrahedral mesh and hexahedral mesh are combined, the mesh is encrypted at nozzles and triangular prisms, and an expansion layer is set up at the outflow field. Finally, the scenes of the mesh is observed to be about 0.2, and the mesh quality measurement grade is shown in Table 1 [32], which shows that it belongs to the category of “very good.” The orthogonal mass is about 0.9, and the numerical range of orthogonal mass is 0~1; the closer to 1, the better. The above shows that the lattice quality meets the requirements [32]. The divided mesh is shown in Figure 4.

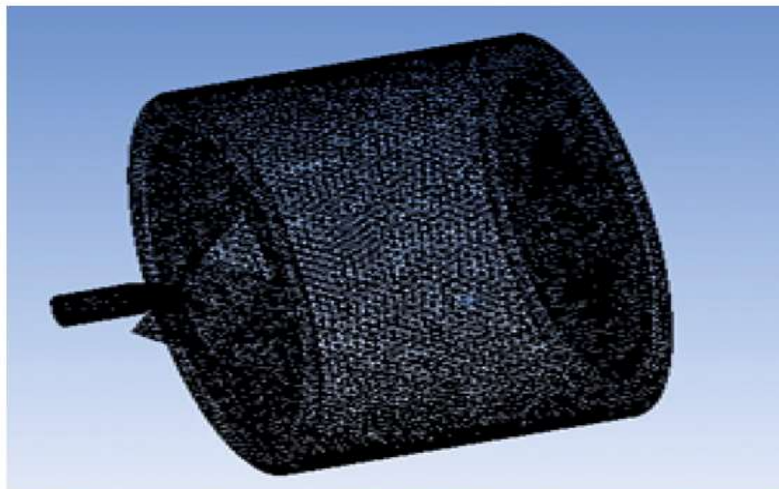


Figure 6 : Mesh model of nozzle and external flow field.

The boundary condition setting is shown in Figure 3. Since air fills the whole outflow field in the initial state, air is selected as the main phase and water fluid as the second phase in order to solve the near-real situation. Select the inlet boundary pressure of the nozzle to be 6–12 MPa, and set the volume fraction of inlet water to be 1, i.e., the nozzle is filled with water in the initial state, the outlet pressure is set to 1 atmosphere (i.e., the relative static pressure is zero), and the external flow field is filled with air at the beginning of injection. The wall surface adopts the standard nonslip wall surface, the standard wall surface function simulates the near-wall effect, and the SIMPLE pressure-velocity coupling semi-implicit algorithm is used to solve the problem. The jet medium is water, the density at room temperature is  $998 \text{ kg/m}^3$ , and the dynamic viscosity is  $0.001 \text{ kg/(m}\cdot\text{s)}$ . The air density is  $1.225 \text{ kg/m}^3$ , and the dynamic viscosity is  $1.789 \text{ kg/(m}\cdot\text{s)}$  [33]. After setting the boundary conditions, the first-order upwind discrete scheme is used to solve the problem. In order to make the calculation more accurate, the monitoring accuracy is adjusted to 0.0001, and the number of iteration steps is set to 1000 steps. After 1000 steps, the residual tends to be stable and the operation is finished.

### Verify the Correctness of the Model

For continuous jet, the Bernoulli equation is adopted between the inner and outer two points of nozzle outlet cross section, ignoring the height difference between the two points, and the following relation [34] can be obtained: where  $p_1$  and  $p_2$  are the static pressure inside and outside the nozzle; and are the average flow velocity inside and outside the nozzle.

Applying the continuous equation to two points, the following relation can be obtained: For the convenience of theoretical analysis, the nozzle flow path can be a circular tube structure; that is,  $A = \pi d^2/4$ ; assuming  $\rho_1 = \rho_2$ , the following relationship can be deduced by combining (5) and (6):

For the water jet used for washing, because  $p_1 \gg p_2$ ,  $(d_2/d_1)^4 \ll 1$ , and  $\rho = 998 \text{ kg/m}^3$ , the relevant values are substituted into (7), and the simplified expression of jet velocity is obtained: where  $p$  is the static pressure at the nozzle inlet; is the nozzle outlet velocity.

From equation (8), when the static pressure at the inlet is 8 MPa, the velocity at the outlet of the nozzle is 126.60 m/s.

In order to verify the correctness of the simulation model, it is necessary to compare the value calculated by the above formula with the simulation result. Therefore, both solutions are set as the static inlet pressure 8 MPa. The simulation results are as shown in Figure 5. The velocity at the nozzle outlet is 127.40 m/s according to the velocity nephogram. The error  $\Delta = (127.4 - 126.6)/126.6 = 0.632\%$ . The simulation results are very close to the theoretical calculation results, which show that the model is reliable.

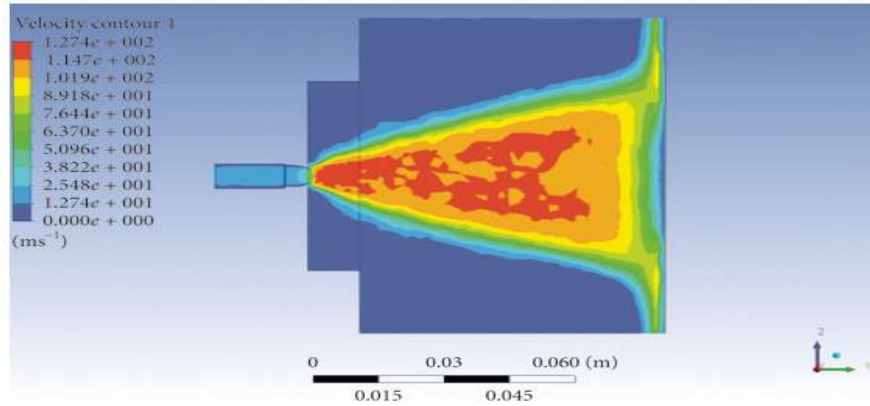


Figure 7: Water jet velocity reprogram with inlet pressure of 8 MPa.

## Results and Discussion

### Simulation Analysis and Comparison of Different Target Distances

As can be seen from Figure , the water jet velocity and dynamic pressure in the basic section gradually decrease with the axial target distance (the distance from the nozzle outlet to the automobile surface). Obviously, the choice of target distance has a great influence on the washing effect. The dynamic pressure on the target surface is an important characteristic of water jet, which represents the striking force of water jet on the target surface.

The inlet pressure is selected to be 8 MPa, and the external flow field is simulated and analyzed under the conditions that the target distances are 60 mm, 70 mm, 80 mm, and 100 mm, respectively. The dynamic pressure cloud images of the target surface under different target distances are obtained as shown in Figure, and the radial dynamic pressure curves of the target surface under different target distances.

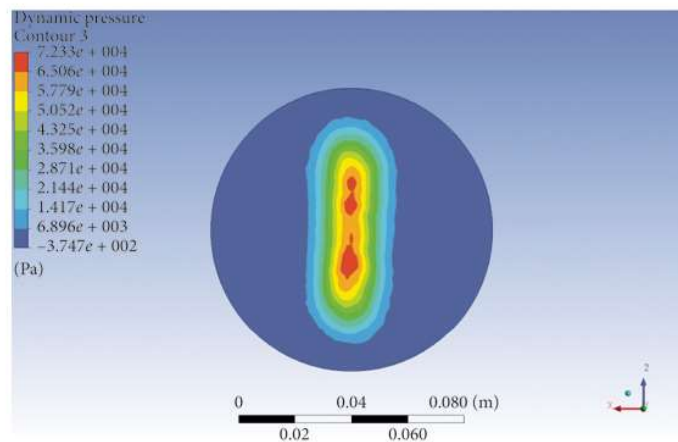


Figure 8: Dynamic pressure reprogram of target surface at different target distances.



In order to achieve the best washing effect, the dynamic pressure on the target surface should be as large as possible. As can be seen from Figure these dynamic pressures vary significantly under the same inlet pressure and different target distances. When the target distances are 60 mm, 70 mm, 80 mm, and 100 mm, the corresponding maximum dynamic pressure values at the target center are 125400 Pa, 111300 Pa, 96170 Pa, and 72330 Pa, respectively. Although the washing capability of the water jet decreases with larger target distance, the coverage area of the water jet increases, and the area of the automobile that can be cleaned increases. By observing Figures, it can be seen that when the target distance is 60 mm, the water jet reaching the target surface has a reverse impact force that partially cancels the forward water jet reaching the target surface due to the nozzle being too close to the surface of the automobile, making the dynamic pressure on the target surface uneven.

### Different Inlet Pressures

The target distance is 70 mm, and the external flow field is simulated under the conditions of inlet pressures of 6 MPa, 8 MPa, 10 MPa, and 12 MPa, respectively. The dynamic pressure nephogram of the target surface under different inlet pressures is obtained as shown in Figure, and the axial velocity distribution under different inlet pressures is shown in Figure .

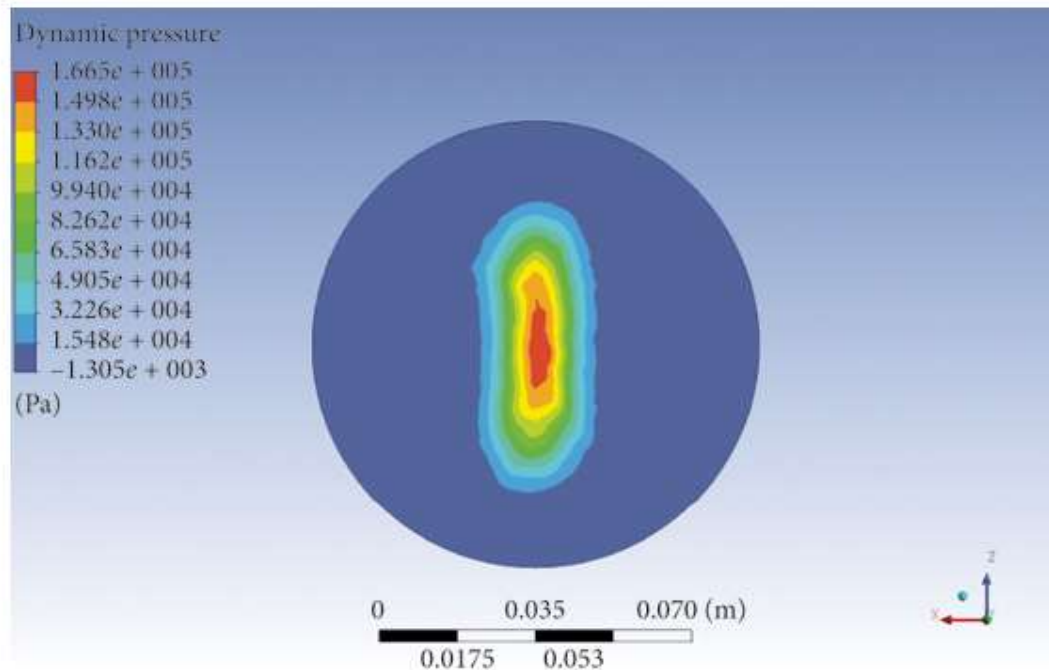


Figure 9: Target dynamic pressure reprogram under different inlet pressure.

As can be seen from Figure, when the inlet pressure changes from 6 MPa to 8 MPa, the target surface dynamic pressure increase rate is 33.18%, when the inlet pressure changes from 8 MPa to 10 MPa, the target surface dynamic pressure increase rate is 24.89%, and when the inlet pressure changes from 10 MPa to 12 MPa, the target surface dynamic pressure increase rate is 19.78%. It can be concluded that the increase rate of the dynamic pressure on the target surface decreases with the increase of the inlet pressure; under the condition of a certain target distance, the area covered by water jets with different inlet pressures is basically the same. As seen in Figure when the inlet pressure starts to increase from 6 MPa, the axial speed also increases. The speed increase from 6 MPa to 8 MPa is larger than that of from 8 MPa to 10 MPa or 10 MPa to 12 MPa. Comparing with the speed before reaching the target surface, it can be seen that the decay speed of the axial speed before reaching the target surface becomes faster with the increase of the inlet pressure. Therefore, considering the dynamic pressure of the target surface and the axial speed, the inlet pressure is 10 MPa as the optimal pressure under this working condition. In conclusion, when the target distance is fixed, the coverage area of water jet has nothing to do with the inlet pressure; with the increase of inlet pressure, the dynamic pressure and axial velocity of the target increase continuously, but their increasing rate decreases.

### **Comparison of Different Included Angles**

At present, the spray rod nozzle of the car wash is perpendicular to the surface of the automobile, so that the surface of the automobile is mainly subject to normal strike force and little tangential strike force during the washing process, and some stubborn stains are not easy to be cleaned off. In the process of water jet washing, it should be considered that inclining the jet direction of the nozzle to the target surface (automobile surface) at a certain angle will greatly enhance its washing effect. At this time, the cleaned surface is affected by the impact forces and shear forces of the water jet. When the water jet hits the target surface, the velocity is decomposed into two directions perpendicular to the target surface and parallel to the target surface. The velocity perpendicular to the target surface will strike and loosen the attachments on the target surface, and the velocity parallel to the target surface will wash away the attachments.

In order to realize the simulation of outflow field under different included angles, the normal included angles between nozzle and target surface are  $0^\circ$ ,  $15^\circ$ ,  $30^\circ$ , and  $45^\circ$  through different angles of target surface inclination. The schematic diagram of the model is shown in Figure, and the 3D model is shown in Figure .

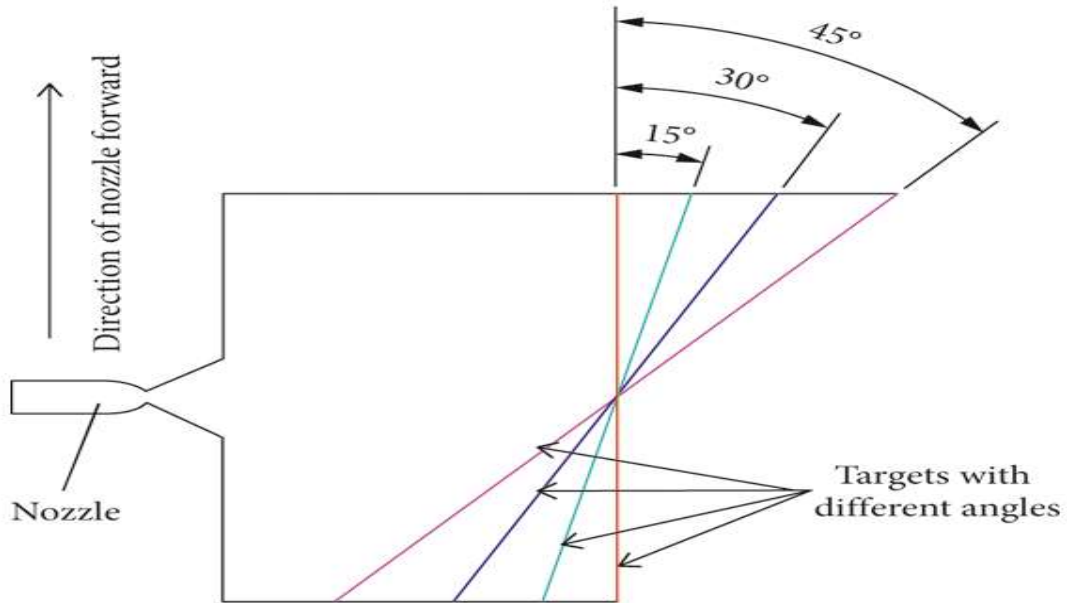


Figure 10: Model schematic diagram different from normal angle of target surface

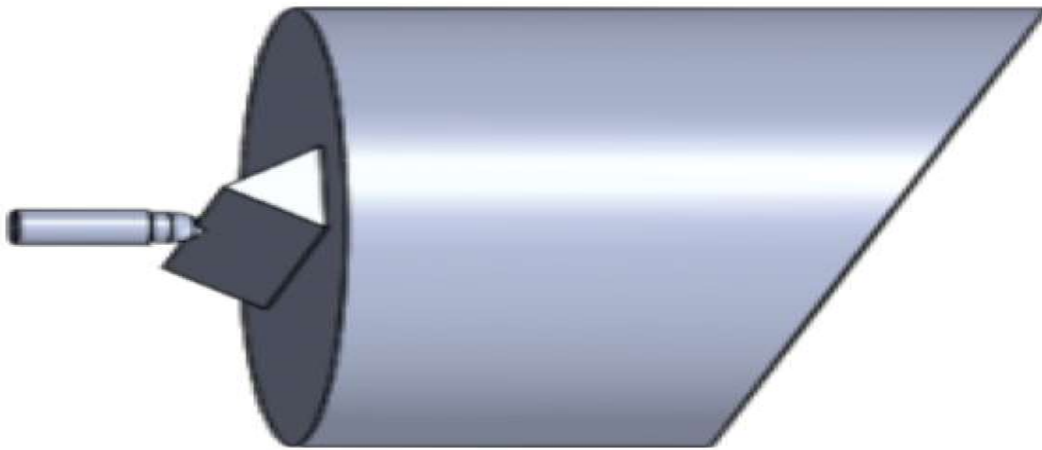


Figure 11 :3D model with inclined angle.

As can be seen from Figure, regardless of the inlet pressure, the following conclusions can be drawn. The dynamic pressure of the target surface decreases with the increase of the inclination angle. From  $15^\circ$  to  $30^\circ$ , the decreased amplitude is small, but from  $30^\circ$  to  $45^\circ$ , the decrease amplitude increases. This is due to the fact that part of the kinetic energy is absorbed by the target surface after the water jet impacts the target surface at a certain angle, and the other part of the kinetic energy produces a tangential force on the stain, resulting in a decrease in the dynamic pressure on the normal target surface. By observing Figure it can be seen that when the inclination angle is  $0^\circ$ , the speed of the water jet reaching the target surface in the tangential advancing direction is very small. After inclining by a certain angle, the speed of the water jet

reaching the target surface in the tangential advancing direction of the nozzle gradually increases and reaches the maximum when the inclination angle is 30°. Therefore, considering the velocity distribution and the dynamic pressure of the target surface comprehensively, 30° is taken as the optimal included angle.

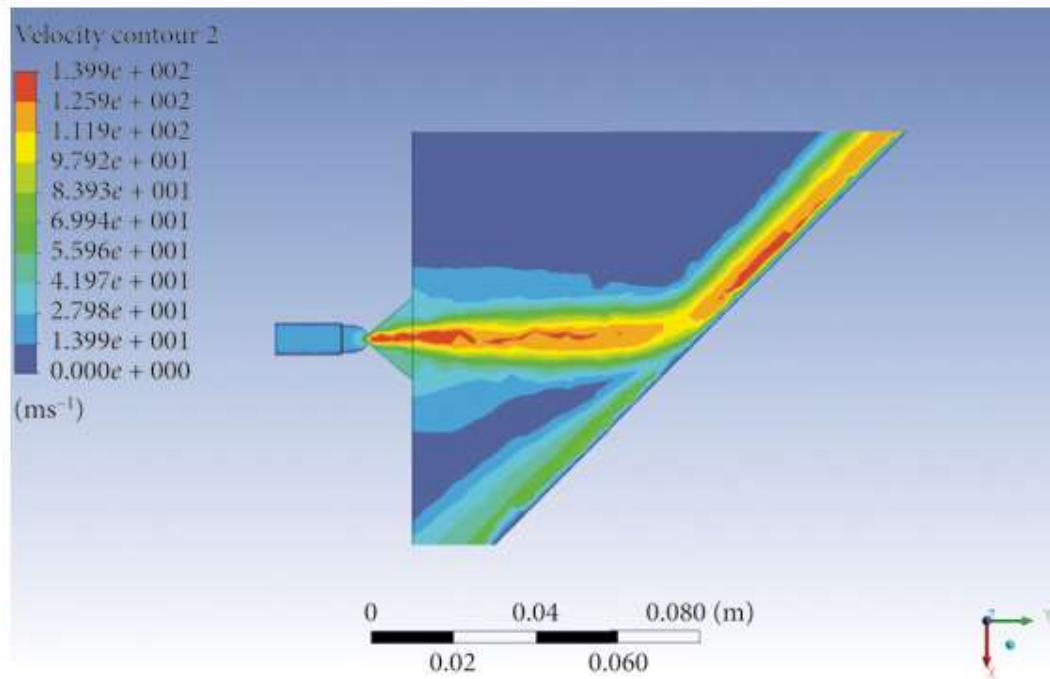


Fig. 12: Velocity reprogram at different angles. (a) 0°. (b) 15°. (c) 30°. (d) 45°.

### Comparison of Simulation Analysis with Different Spacing

When arranging nozzles, the influence of nozzle spacing on the external flow field should be considered. If the nozzle spacing is too small, the edge water jet of the fan-type external flow field will interfere, thus affecting the washing effect. If the nozzle spacing is too large, the fan-type outflow field cannot cover all washing surfaces and cannot meet the washing requirements. In this paper, the nozzle spacing is simulated by establishing a 3D model as shown in Figure

When the nozzle spacing is 100 mm, the watersheds of the two nozzles hardly intersect, so that some areas of the automobile surface between the two nozzles cannot be effectively cleaned. With the decrease of the nozzle spacing, the outflow fields of the two nozzles begin to intersect, so that the target surface between the two nozzles can be effectively cleaned. By looking at Figure 17, it is shown that, with the decrease of nozzle spacing, the interference degree of adjacent water jets increases gradually. Therefore, considering the velocity distribution and the dynamic pressure on the target surface, it is more appropriate to select the nozzle spacing of

70 mm under this working condition. The above results show that the target distance and nozzle distance must be matched to ensure the washing effect. It is necessary to discuss the relationship between the target distance and nozzle distance.

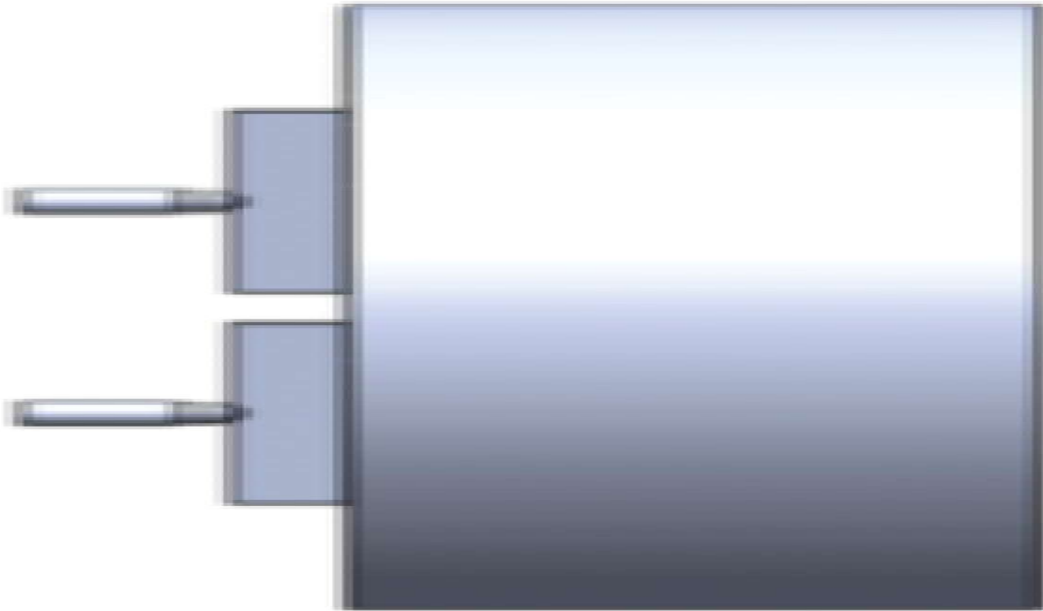
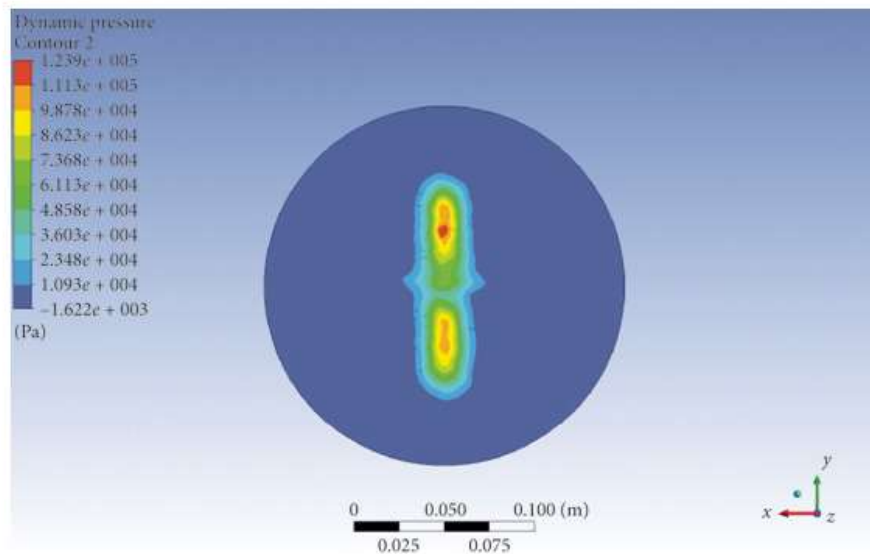


Figure 13: 3D model with different spacing.



(d)Figure 14: Dynamic pressure echograms of target surfaces with different spacing. (a) 100 mm. (b) 80 mm. (c) 70 mm. (d) 60 mm.

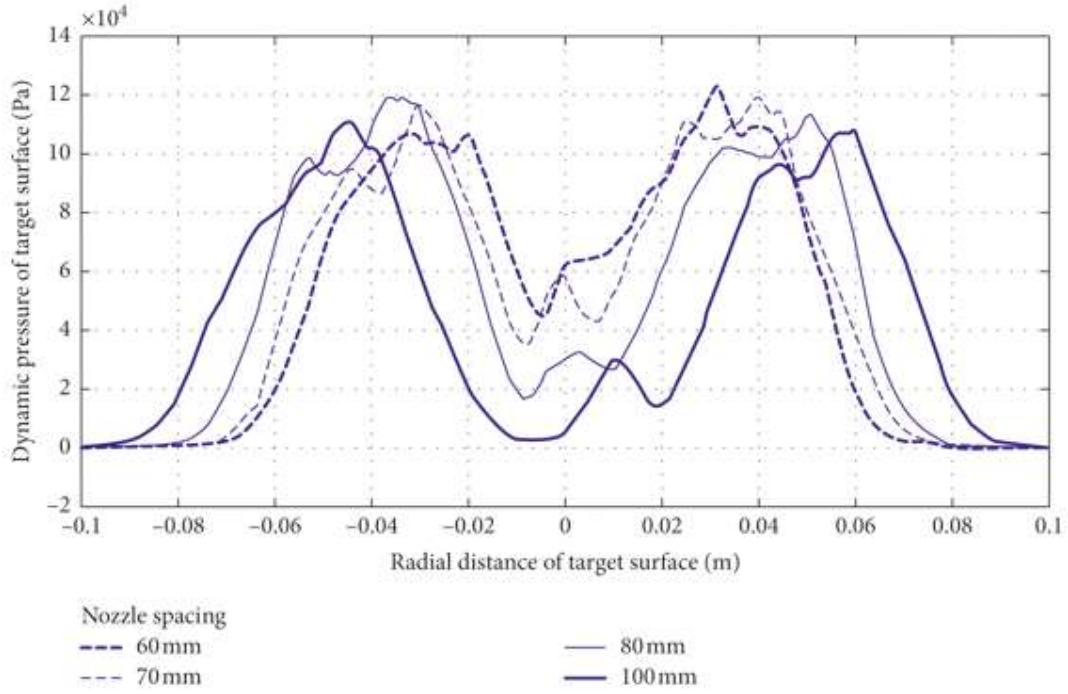


Figure 15: Radial dynamic pressure of target surface at different spacing.

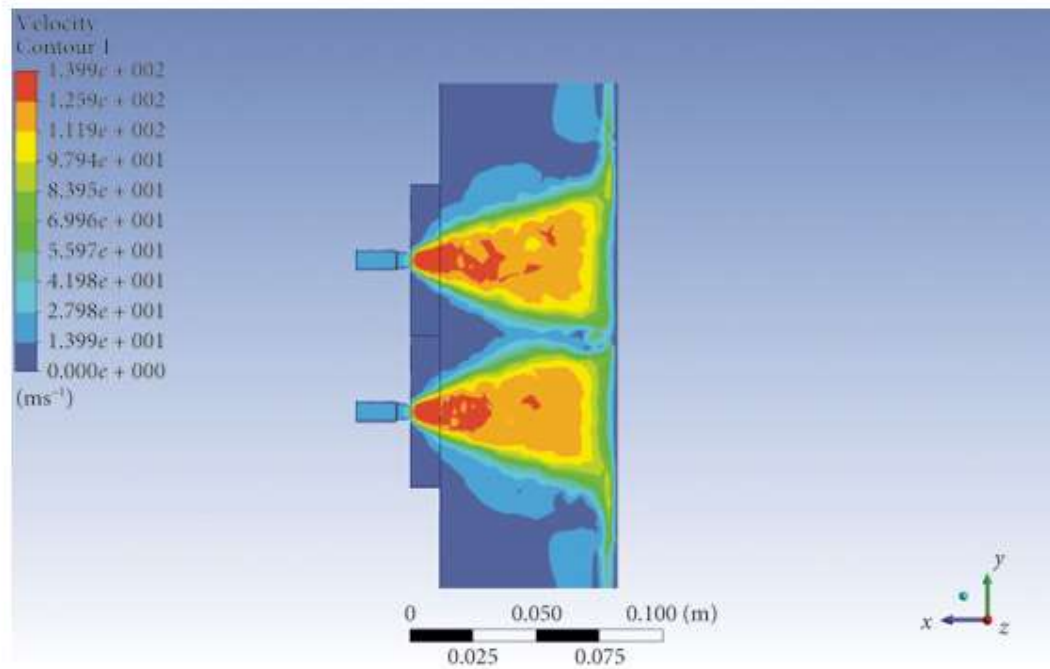


Figure 14\6 : Velocity nephogram with different spacing. (a) 100 mm. (b) 80 mm. (c) 70 mm. (d) 60 mm.

### Shooting Width under Different Jet Angles

As can be seen from Figure 8, the inlet pressure of the nozzle has little influence on the shooting width (range covering the target surface) of the water jet. As can be seen from Figures 15 and 16, the target distance has a great influence on the shooting width (range covering the target surface) of the water jet. In addition, practical application and theoretical analysis show that the jet angle  $\alpha$  of the nozzle will inevitably affect the jet width of the water jet (covering the range of the target surface). Based on the above model, this paper discusses the relationship between target distance and shooting width under different jet angles by numerical simulation. When the jet angle  $\alpha$  is  $15^\circ$ ,  $30^\circ$ ,  $45^\circ$ , and  $60^\circ$  and the target distance is adjusted to 50 mm, 100 mm, 150 mm, 200 mm, 250 mm, 300 mm, 350 mm, 400 mm, 450 mm, and 500 mm, respectively, the shooting width is investigated to find out the matching relationship between the target distance and the shooting width. The solution result is shown in Figure 18.

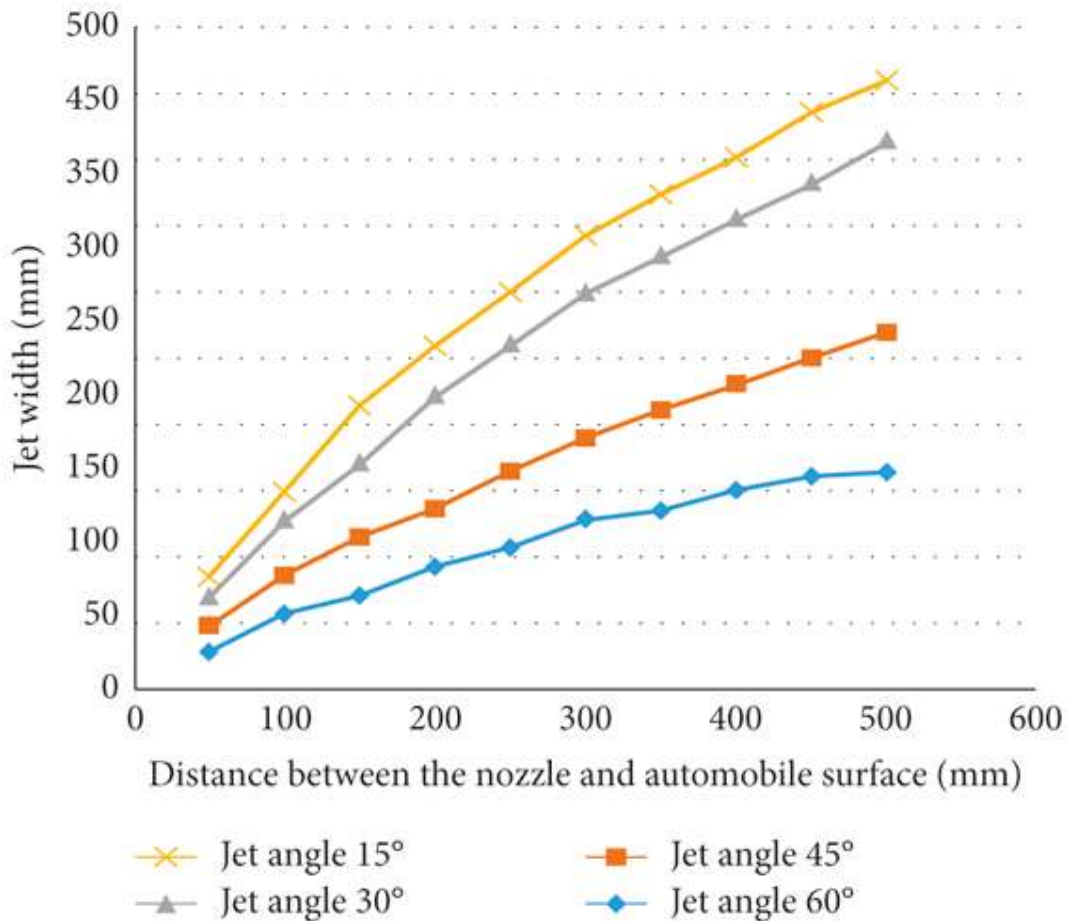


Figure 17 : Relationship curve between jet target distance and jet width under different jet angles.

From the solution rule curve in Figure , it can be seen that no matter what the jet angle is, the width of the water jet will increase with the increase of the target distance. When the jet angle is small, the increase rate of jet width is small, and the increase rate also increases with the increase of jet angle, but the increase rate tends to be stable when the jet angle is greater than or equal to  $45^\circ$ . Only when the nozzle spacing is less than or equal to the jet width, the whole automobile surface can be completely covered by the water jet to ensure that the automobile is completely cleaned. However, Figure can be used as the theoretical basis for matching the jet angle, nozzle spacing, and the distance between the nozzle and the automobile surface (target distance). In actual automobile washing, the nozzle spacing on the spray rod is generally premade (it will not change during automobile washing). If the nozzle spacing is too small, the jet coverage area can be effectively increased, but the number of nozzles on the spray rod of the same length will inevitably increase and the water consumption will also rise sharply. As can be seen from Figure, when the nozzle spacing is too large, part of the automobile surface cannot be covered by water jet. Therefore, when washing the car, the distance (target distance) between the nozzle on the spray rod and the surface of the automobile can be adjusted to ensure that the jet width value is always greater than the nozzle spacing, thus achieving the purpose of washing without dead corners. For the automatic automobile washer, the regular curve in Figure 18 can be input into the electronic control integrated control module, and dynamically adjusting the distance (target distance) between the spray rod and the automobile not only makes the automobile surface fully covered and cleaned but also ensures less jet interference from adjacent nozzles and no waste of water.

### Conclusion

The distance between the target surfaces should be determined by comprehensively considering the uniformity of the dynamic pressure on the target surface and keeping the target surface with large dynamic pressure. Although the larger the target distance, the weaker the washing ability of the water jet, the larger the coverage area of the water jet, the larger the area of the automobile that can be cleaned.(2)With the increase of inlet pressure, the dynamic pressure on the target surface and the axial velocity will increase, but the growth rate will gradually decrease when reaching a certain pressure. Under the condition of a certain target distance, the area covered by water jets with different inlet pressures is basically the same.(3)After the nozzle and the normal line of the automobile surface are inclined at a certain angle, the target surface is affected not only by normal striking force but also by tangential force, which makes stains easier to remove. Through simulation analysis, it is found that the optimal angle is to tilt the nozzle and the normal line of the automobile  $30^\circ$ .(4)The target distance and nozzle distance must be matched; otherwise, it will lead to two extreme situations: one is that the automobile surface is not covered by water jet; the other case is that the water jets of adjacent nozzles interfere seriously with each other and the washing efficiency is reduced. Through numerical simulation, the matching curves among jet angle, nozzle spacing, and the distance between nozzle and automobile surface (target distance) are obtained, which provides a basic theoretical basis for the optimal design of automatic automobile washing.(5)Through industrial tests, the correctness of the above research conclusions is verified.



## References

1. K. Jiang, F. Yan, and H. Zhang, “Data-driven modeling and UFIR-based outlet NO<sub>x</sub> estimation for diesel-engine SCR systems,” *IEEE Transactions on Industrial Electronics*, vol. 67, no. 6, pp. 5012–5021, 2022.
2. K. Jiang, F. Yan, and H. Zhang, “Hydrothermal aging factor estimation for two-cell diesel-engine SCR systems via a dual time-scale unscented Kalman filter,” *IEEE Transactions on Industrial Electronics*, vol. 67, no. 1, pp. 442–450, 2022.
3. M. Kierzkowski and H. Law, “Car wash noise and EPA regulation—a case study,” in *Proceedings of the ACOUSTICS 2017 Perth: Sound, Science and Society—2017 Annual Conference of the Australian Acoustical Society, AAS 2017*, Perth, Australia, November 2017.
4. A. Nair and S. Kumanan, “Optimization of size and form characteristics using multi-objective grey analysis in abrasive water jet drilling of Inconel 617,” *Journal of the Brazilian Society of Mechanical Sciences and Engineering*, vol. 40, no. 3, pp. 1–15, 2018.
5. S. Thomas, M. Antony, and T. Dimitra, “Hard rock cutting with high pressure jets in various ambient pressure regimes,” *International Journal of Rock Mechanics and Mining Sciences*, vol. 108, no. 8, pp. 179–188, 2018.
6. D. Hu, X.-H. Li, C.-L. Tang, and Y. Kang, “Analytical and experimental investigations of the pulsed air-water jet,” *Journal of Fluids and Structures*, vol. 54, pp. 88–102, 2015.
7. S. Hannes, K. Hannes, M. Marc, and J. P. Majschak, “Investigations to increase washing efficiency with pulsed liquid jet,” *Chemie Ingenieur Technik*, vol. 86, no. 5, pp. 707–713, 2014.
8. L. M. Hlaváč, “Application of water jet description on the de-scaling process,” *International Journal of Advanced Manufacturing Technology*, vol. 80, no. 5–8, pp. 721–735, 2015.
9. F. Enrico, K. Sebastian, and S. Enrico, “Effect of industrial scale stand-off distance on water jet break-up, washing and forces imposed on soil layers,” *Food and Bioproducts Processing*, vol. 113, no. S1, pp. 129–141, 2019.
10. E. Helal, F. S. Abdelhaleem, and W. A. Elshenawy, “Numerical assessment of the performance of bed water jets in submerged hydraulic jumps,” *Journal of Irrigation and Drainage Engineering*, vol. 146, no. 7, 2020.
11. A. Janardanan, P. C. Ajil, P. Anju, T. V. Eldiya, and D. Davis, “Android application for car wash services,” in *Proceedings of 1st International Conference on Emerging Trends and Innovations in Engineering and Technological Research*, Cochin, India, July 2018.
12. D. Phipps, R. Alkhaddar, and M. Stiller, “Water saving in domestic car washing,” in *Proceedings of World Environmental and Water Resources Congress 2013: Showcasing the Future*, Cincinnati, OH, USA, May 2013.
13. T. T. Yu, J. Q. Wang, L. T. Wu, and Y. Xu, “Three-stage network for age estimation,” *CAAI Transactions on Intelligence Technology*, vol. 4, no. 2, pp. 122–126, 2019.
14. R. Jiang, H. Zhou, H. Wang, and S. S. Ge, “Maximum entropy searching,” *CAAI Transactions on Intelligence Technology*, vol. 4, no. 1, pp. 1–8, 2019.
15. C. L. Tang, D. Hu, and F. H. Zhang, “Study on the frequency characteristic of self-excited oscillation pulsed water jet,” *Advanced Materials Research*, vol. 317–319, pp. 1456–1461, 2011.
16. E. Fuchs, H. Köhler, and J. P. Majschak, “Measurement of the impact force and pressure of water jets under the influence of jet break-up,” *Chemie Ingenieur Technik*, vol. 91, no. 4, pp. 455–466, 2019.

17. J. W. Wen, Z. W. Qi, and S. S. Behbahani, "Research on the structures and hydraulic performances of the typical direct jet nozzles for water jet technology," *Journal of the Brazilian Society of Mechanical Sciences and Engineering*, vol. 41, no. 12, p. 570, 2019.
18. P. A. Dumbhare, S. Dubey, Y. V. Deshpande, A. B. Andhare, and P. S. Barve, "Modelling and multi-objective optimization of surface roughness and kerf taper angle in abrasive water jet machining of steel," *Journal of the Brazilian Society of Mechanical Sciences and Engineering*, vol. 40, no. 5, pp. 1–13, 2018.
19. J. W. Wen, C. Chen, and U. Campos, "Experimental research on the performances of water jet devices and proposing the parameters of borehole hydraulic mining for oil shale," *PLoS One*, vol. 13, no. 6, Article ID e0199027, 2018.
20. M. Nadeem, N. Q. Tri, C. Diallo, and U. Venkatadri, "Contribution to spraying nozzle study: a comparative investigation of imaging and simulation approaches," *Pakistan Journal of Agricultural Sciences*, vol. 56, no. 1, pp. 215–224, 2019.
21. M. Nadeem, Y. K. Chang, U. Venkatadri, C. Diallo, P. Haward, and T. Nguyen-Quang, "Water quantification from sprayer nozzle by using particle image velocimetry (PIV) versus imaging processing techniques," *Pakistan Journal of Agricultural Sciences*, vol. 55, no. 1, pp. 203–210, 2018.
22. E. Fuchs, M. Helbig, M. Pfister, and J.-P. Majschak, "Erhöhung der Reinigungseffizienz bei der Cleaning-in-place-Reinigung durch diskontinuierliche Flüssigkeitsstrahlen," *Chemie Ingenieur Technik*, vol. 89, no. 8, pp. 1072–1082, 2017.
23. M. W. L. Chee, T. V. Ahuja, R. K. Bhagat et al., "Impinging jet cleaning of tank walls: effect of jet length, wall curvature and related phenomena," *Food and Bioprocesses Processing*, vol. 113, no. S1, pp. 142–153, 2019.
24. B. S. Nie, H. Wang, L. Li, and J. Zhang, "Numerical investigation of the flow field inside and outside high-pressure abrasive waterjet nozzle," in *Proceedings of 1st International Symposium on Mine Safety Science and Engineering, ISMSSE 2011*, Beijing, China, October 2011.
25. A. Kermanpur, A. Ebnonnasir, and M. Hedayati, "A novel analytical-artificial neural network model to improve efficiency of high pressure descaling nozzles in hot strip rolling of steels," *Materials Science and Technology*, vol. 23, no. 8, pp. 951–957, 2007.
26. A. Kermanpur, A. Ebnonnasir, A. R. K. Yeganeh, and J. Izadi, "Artificial neural network modeling of high pressure descaling operation in hot strip rolling of steels," *ISIJ International*, vol. 48, no. 7, pp. 963–970, 2008.
27. Y. T. Dou, M. Zhou, and X. J. Cai, "Nozzle arrangement of self-propelled pipeline washing nozzle," *Oil and Gas Storage and Transportation*, vol. 38, no. 6, pp. 662–666, 2019.
28. C. T. Liu, G. Liu, and Z. X. Yan, "Study on cleaning effect of different water flows on the pulsed cavitating jet nozzle," *Shock and Vibration*, vol. 2019, Article ID 1496594, 15 pages, 2019.
29. B. J. Liang and D. R. Gao, "Optimization of structural parameters of fan-shaped high-pressure nozzle," *Journal of Drainage and Irrigation Machinery Engineering*, vol. 38, no. 1, pp. 69–75, 2020.
30. Y. Liu, Q. B. Ba, L. P. He, K. Shen, and W. Xiong, "Study on the rock-breaking effect of water jets generated by self-rotatory multinozzle drilling bit," *Energy Science and Engineering*, vol. 8, no. 7, pp. 2457–2470, 2020.

31. Y.-Y. Zhang, *Fluid Mechanics*, Higher Education Press, Beijing, China, 2015.
32. H. Kun and L. Zhenbei, *Detailed Explanation of ANSYS ICEM CFD Engineering Example*, Posts and Telecom Press, Beijing, China, 2014.
33. J. Bingbing, Z. Xiaoxia, and G. Yan, *ANSYS ICEM CFD Basic Course and Example Explanation*, China Machine Press, Beijing, China, 2015.
34. K. Jin, "Design and experiment research of ultrahigh pressure water jet boom washing device," Master's thesis, Dalian Maritime University, Dalian, China, 2018, in Chinese.